



Preparation and study of the catalytic application in the synthesis of xanthenedione pharmaceuticals of a hybrid nano-system based on copper, zinc and iron nanoparticles

Mir Saeed Esmaeili¹ · Zahra Varzi¹ · Reza Taheri-Ledari¹ · Ali Maleki¹

Received: 30 June 2020 / Accepted: 23 October 2020
© Springer Nature B.V. 2020

Abstract

A novel efficiently mixed transition metal oxides catalytic system with high catalytic activity and heterogeneity constructed of copper and zinc oxide nanoparticles is presented. For preparation of this hybrid catalytic system, carrageenan as a natural polymeric matrix has been chosen to add biocompatibility to the heterogeneous catalyst. Then, the carrageenan textures have been magnetized through the composition with iron oxide nanoparticles. Copper and zinc metallic sites are employed as the main catalytic sites for catalyzing the synthesis of xanthenedione pharmaceutical derivatives from aldehyde and dimedone. Due to the magnetic behavior of the catalyst, the purification process is carried out with high convenience. Herein, a plausible mechanism for the catalytic process is suggested and reusability of the presented catalyst is also investigated. In this report, it has been well-proven that high reaction yields are obtained for xanthenedione derivatives under mild conditions, through applying the presented hybrid catalytic system.

Keywords Metal oxides · Solid-phase catalyst · Copper nanoparticle · Pharmaceutical compounds · Zinc ferrite

Zahra Varzi is a Co-first author.

Electronic supplementary material The online version of this article (<https://doi.org/10.1007/s11164-020-04311-8>) contains supplementary material, which is available to authorized users.

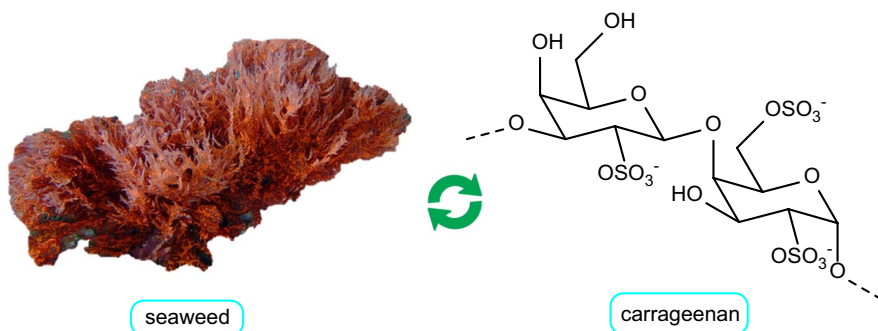
✉ Ali Maleki
maleki@iust.ac.ir

¹ Catalysts and Organic Synthesis Research Laboratory, Department of Chemistry, Iran University of Science and Technology (IUST), 16846-13114 Tehran, Iran

Introduction

Active pharmaceutical ingredients (APIs) typically include complex chemical structures that are difficult to be synthesized. Besides, they include several heteroatoms such as nitrogen and oxygen at their structures, which provide a suitable situation for catalytic activations [1, 2]. Metals are usually used in the structure of the heterogeneous catalytic systems that create effective electronic interactions with the lone pair electrons and lead to the facile synthesis processes [3–7]. Recently, several works have been reported about the preparation and application of the metallic nanocatalysts for facilitating the synthesis of the APIs with complex structures [8–10]. For instance, palladium-decorated hybrid nanocatalysts have been widely reported for this purpose [11–15]. Transition metals such as copper, palladium, zinc, manganese, silver, gold, iron, and metal oxides have also been used for catalyzing the chemical synthesis reactions and other purposes [16–23]. In this regard, we intended to design a novel transition metal-containing heterogeneous catalytic system, and suitably apply that for facilitating the synthesis of xanthenedione pharmaceutical derivatives [24, 25]. In this way, we use zinc, copper, and iron metals for preparation of a nanosized hybrid system. In fact, zinc ferrite is used as the magnetic agent in the composite and provides a substantial property for the catalyst to be conveniently isolated from the reaction mixture and reused again for the several times [26], whereas copper(I) oxide nanoparticles are the main catalytic active sites and play the key role in the catalytic process [27]. From pharmacological aspect, xanthenedione is considered as a substantial antioxidant and also as an appropriate inhibitor for acetylcholinesterase (AChE) enzyme [28]. The chemical structure of xanthenedione includes oxygen atoms coming from the aldehyde and dimedone (5,5-dimethylcyclohexane-1,3-dione), as the initial structural units. So, metal atoms could catalyze the synthetic process of xanthenedione through forming effective electronic interactions with these oxygen atoms. In this regard, several metallic systems including iron, lead, zirconium, zinc, and natural structures have been prepared and used [29–31].

Heterogeneous catalytic systems are generally preferred due to their convenient separation from the reaction mixture [32–34]. Recently, the magnetic property of the catalytic systems has attracted so much attentions because they could be separated by using an external magnet and also the catalyst is recycled and reused for several times [35, 36]. For magnetization of the catalytic systems, zinc ferrite and iron oxide nanoparticles (Fe_2O_3 , Fe_2O_4 , and Fe_3O_4 NPs) are usually used [37, 38]. Super-paramagnetic behavior of the zinc ferrite and iron oxide NPs has led researchers to extensively use that for catalytic applications [39–41]. Previously, we have reported several novel catalytic systems made of iron oxide NPs [42–50]. For this aim, a combination of the zinc ferrite and iron oxide NPs with other materials is prepared. As a well-known strategy, a polymeric matrix is chosen for the composition with magnetic NPs and also immobilization of the metallic NPs [51–57]. In this study, we chose “*carrageenan*” as a natural basis, which is made of a linear sulfated polysaccharides and is extracted from



Scheme 1 Structure of the carrageenan

red edible seaweeds [57]. Since, there are several sulfates and hydroxyl groups in the structure of carrageenan, metallic NPs could be well-immobilized in this natural matrix (Scheme 1). In 2015, Rostamnia and co-workers have reported a magnetic catalytic system based on carrageenan, and used that for clean synthesis of rhodanines [58]. They made a combination of carrageenan and Fe_3O_4 NPs and used the hydroxyl groups of the mentioned composite as the catalytic sites. Here, we intend to use numerous hydroxyl sites of the carrageenan for the formation of the strong H-binding interactions with the metallic sites. These interactions enhance the total stability of the composite. Then, copper(I) ions are distributed onto the surfaces and act as the main catalytic sites, which are more active than the hydroxyl groups. As a desirable result, it is observed that our trimetallic composite results in higher reaction yields in a short time, under green conditions. In this study, firstly, we try to present a convenient preparation route for our hybrid metallic nanocatalyst, including zinc ferrite and copper NPs stabilized in the carrageenan ($\text{Cu-ZnFe}_2\text{O}_4$ @carrageenan nanocomposite). Then, the presented catalytic system is suitably applied for facilitating the synthesis reactions of xanthenedione pharmaceutical derivatives. In this work, this is demonstrated that high reaction yields (98%) are obtained in short reaction time (10 min), under mild reaction conditions, through applying the presented method.

Results and discussion

Preparation of $\text{Cu-ZnFe}_2\text{O}_4$ @carrageenan nanocatalyst

In our designed catalytic system, zinc ferrite has been used as the magnetic agent in the composite and provides a substantial property for catalyst to be conveniently isolated with high convenience. The copper(I) oxide nanoparticles are the main catalytic active sites and play the key role in the catalytic process. In order to prepare the catalytic system, nitrate salts of iron and zinc were co-precipitated in the presence of carrageenan via ultrasonication in a cleaner ultrasound bath, at 50 °C. After well-mixing, the environment of the reaction was gradually alkalized

using a concentrated solution of sodium hydroxide until the color of the mixture was changed to brown, meaning that ZnFe_2O_4 NPs have been well-formed [59]. In our case, sodium hydroxide (0.1 M, 10 mL) was used until $\text{pH} \sim 12$ was obtained. In the next stage, copper(II) chloride was dissolved in a solution of ascorbic acid to form the target $\text{Cu-ZnFe}_2\text{O}_4$ @carrageenan nanocomposite, under reflux conditions (Fig. 1). Here, ascorbic acid plays the role of a reducing agent for Cu^{2+} ions to form Cu_2O NPs, in which Cu is in chemical state Cu^+ .

Characterization of $\text{Cu-ZnFe}_2\text{O}_4$ @carrageenan nanocomposite

To investigate the structure of the prepared $\text{Cu-ZnFe}_2\text{O}_4$ @carrageenan nanocatalyst, Fourier-transform infrared (FT-IR) spectroscopy was used as the first step of characterization. As shown in Fig. 2a, the peak intensity related to hydroxyl groups at $\sim 3400 \text{ cm}^{-1}$ in carrageenan structure has been reduced after the composition of the $\text{Zn/Fe}_2\text{O}_4$ and Cu NPs. It means that the oxygen atoms of the carrageenan have participated in the formation of $\text{Cu-ZnFe}_2\text{O}_4$ @carrageenan composite. Sharp peaks at ~ 1000 and 1200 cm^{-1} coming from the sulfonic acid groups are present in the structure of carrageenan. The intensity of the distinguished peak at $\sim 2900 \text{ cm}^{-1}$ was also reduced. This peak is related to C–H bonds with hybridization sp^3 . Most likely, due to the composition of the metallic NPs with the textures of carrageenan, the vibration of this bond has been a bit lost [60]. Further, the presence of the elements in the structure of ZnFe_2O_4 @carrageenan and $\text{Cu-ZnFe}_2\text{O}_4$ @carrageenan composites were investigated. For this purpose, energy-dispersive X-ray (EDX) spectroscopy was used (Fig. 2b,c). As can be seen, the presence of all the essential atoms is confirmed by the EDX spectra. In addition, a quantitative analysis has been performed showing the weight percentages of the present elements.

The thermal stability and assembly process of the fabricated $\text{Cu-ZnFe}_2\text{O}_4$ @carrageenan composite was studied by thermogravimetric analysis (TGA), in a thermal range of $25\text{--}800 \text{ }^\circ\text{C}$ (Fig. 3a). For the neat carrageenan, proportional to increase

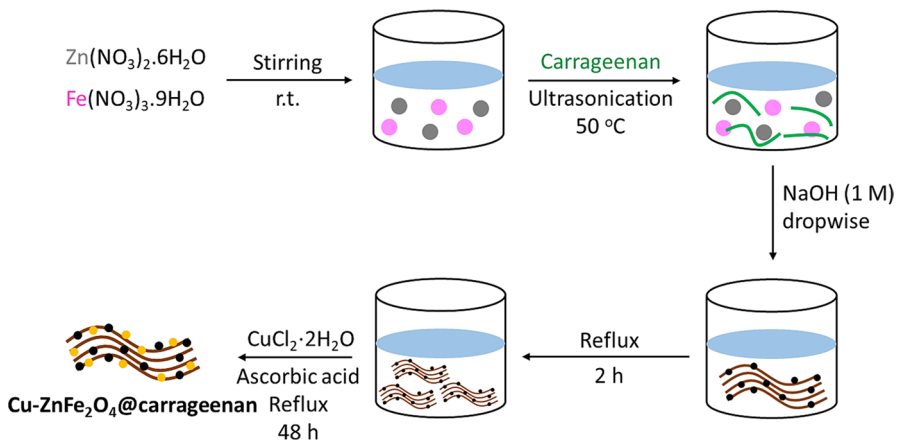


Fig. 1 Schematic of the convenient preparation route of $\text{Cu-ZnFe}_2\text{O}_4$ @carrageenan nanocomposite

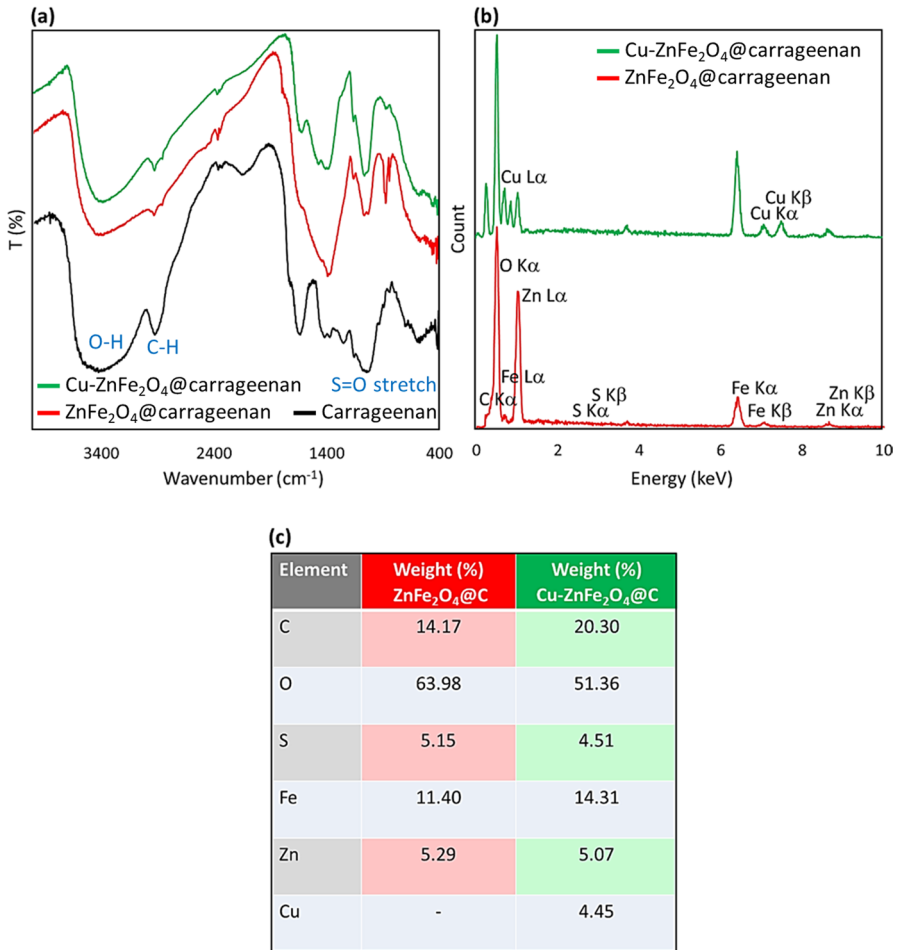


Fig. 2 **a** FT-IR spectra of the neat carrageenan, ZnFe₂O₄@carrageenan, and Cu-ZnFe₂O₄@carrageenan nanocomposite, **b** EDX spectra of ZnFe₂O₄@carrageenan and Cu-ZnFe₂O₄@carrageenan nanocomposite, and **c** EDX quantitative table of the present elements in the structure of Cu-ZnFe₂O₄@carrageenan nanocomposite

the temperature, a partial increase in the weight ratio was observed (ca. 5 wt%) and gradually lost till 100 °C. This fluctuation is likely due to the capability of the carrageenan substrate to adsorb the moisture in the air. During 100–200 °C, about 8% of the total weight has been lost that can be attributed to the removal of the entrapped water molecules in the polymeric matrix [62–64]. Then, the first shoulder has been appeared until ca. 400 °C. According to the literature, in this range, the carrageenan loses its hydroxyl groups via dehydration process and separation of the organic structures like sulfonic acid groups [64]. During this stage, ca. 40% of the weight has been lost [65]. Then, descending trend has been continued to 800 °C. During this stage (400–800 °C), ca. 7% weight loss is observed that is likely coming from

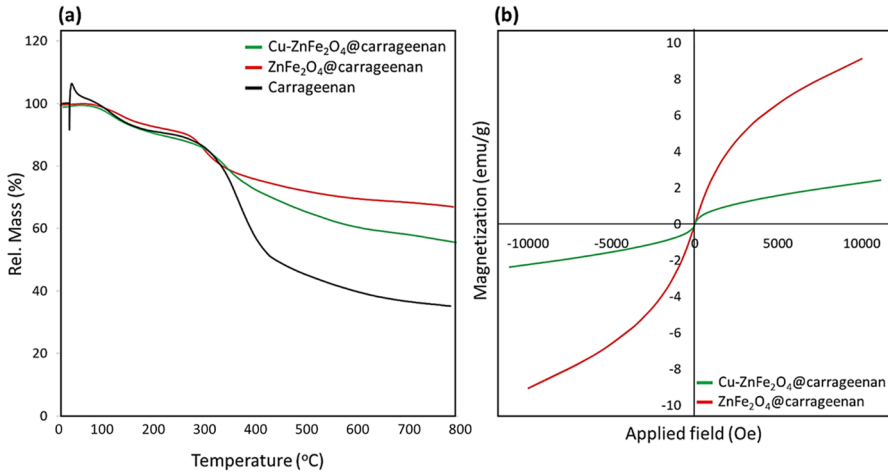


Fig. 3 **a** TGA curves of the neat carrageenan, ZnFe₂O₄@carrageenan, and Cu-ZnFe₂O₄@carrageenan nanocomposite, and **b** VSM *M-H* curves of ZnFe₂O₄@carrageenan and Cu-ZnFe₂O₄@carrageenan nanocomposite at room temperature

the main decomposition of carrageenan, whereas for both ZnFe₂O₄@carrageenan and Cu-ZnFe₂O₄@carrageenan metal composition forms, this is observed that the thermal stability has been increased and the observed degradation in the case of the individual carrageenan (in particular at 300–800 °C) is not observed. The magnetic behavior of the Cu-ZnFe₂O₄@carrageenan composite has been investigated and compared with the ZnFe₂O₄@carrageenan as well (Fig. 3b). As can be seen in the *M-H* curves, the magnetic property was significantly decreased (8.0 emu/g) after copperation of the ZnFe₂O₄@carrageenan composite. As a possible reason, a slight distortion in cubic structure of ZnFe₂O₄ by the Cu ion substitution could be mentioned for the reduced magnetic property. This substitution by the Cu ions may change the magnetization, coercivity and magnetic anisotropy of the ZnFe₂O₄ crystalline structure [66]. However, from this analysis, it was revealed that the particles of the catalyst could be magnetically separated through applying a magnetic field, recycled, and reused.

X-ray diffraction (XRD) pattern of the prepared Cu-ZnFe₂O₄@carrageenan composite was also provided and compared with the reference patterns of ZnFe₂O₄ (JCPDS #001-1109) and Cu₂O (JCPDS #005-0667) (Fig. 4a). As seen in the pattern, a broad peak has been appeared until $2\theta = 20^\circ$ that is attributed to the amorphous structure of carrageenan [67, 68]. Then, the peaks related to the ZnFe₂O₄·NPs, which have been indicated by pink circles, are observed at $2\theta = 30.19^\circ$, 35.47° , 42.94° , 57.12° , and 62.75° . They have been marked in the pattern with Miller indices as (4 0 0), (4 2 2), (6 2 0), (8 0 0), and (7 5 1), respectively. Also, the existence of Cu₂O·NPs has been proven by the peaks that appeared at $2\theta = 22.59^\circ$, 32.48° , 42.41° , and 61.36° . These peaks have been highlighted by blue triangles in the pattern, and also with Miller indices (1 1 1), (2 1 1), (3 1 1), and (4 2 0), respectively. The main indicative peak of Cu₂O·NPs is a sharp peak at ca. 32° . Moreover, to

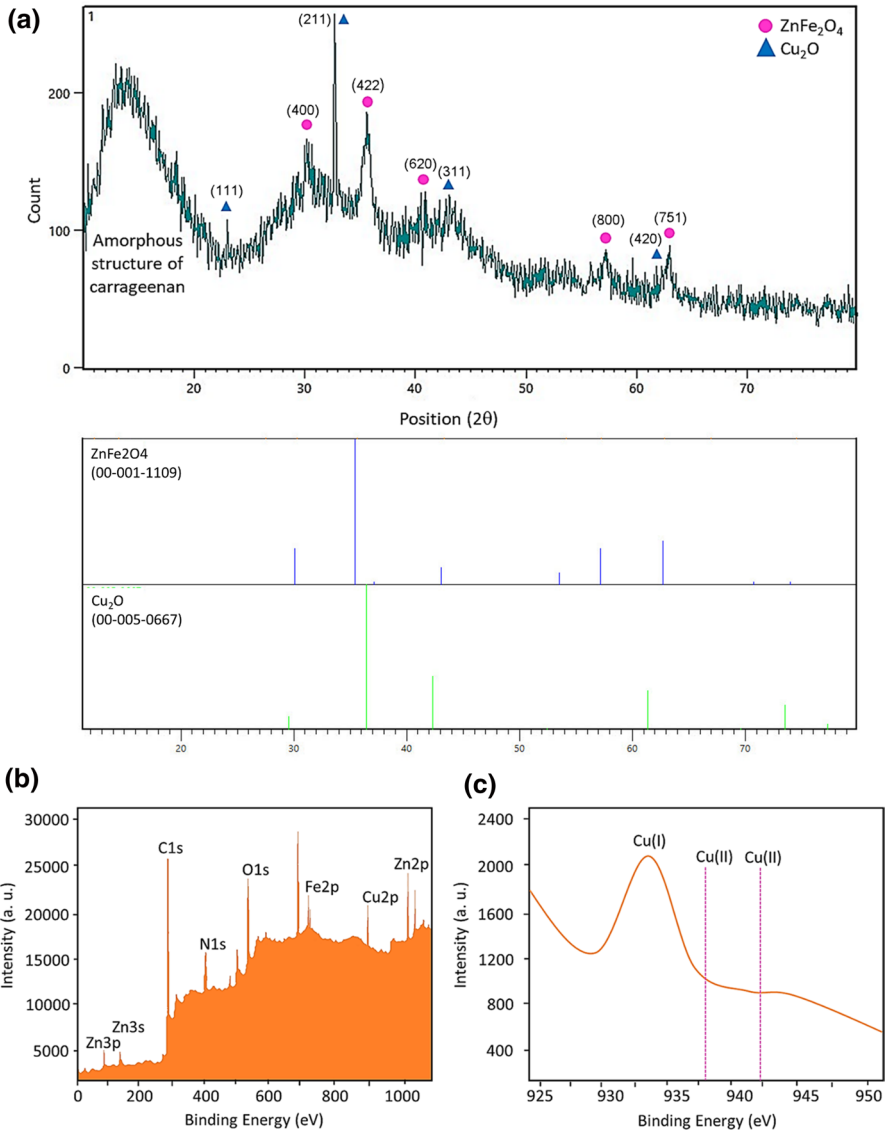


Fig. 4 **a** XRD pattern of the prepared Cu-ZnFe₂O₄@carrageenan nanocomposite, **b** XPS spectrum of the prepared Cu-ZnFe₂O₄@carrageenan, and **c** expanded XPS spectrum in the range of 925–950 eV

prove successful reduction of Cu from chemical state Cu²⁺–Cu⁺, X-ray photoelectron spectroscopy (XPS) was performed [69, 70]. As shown in Fig. 4b, c, a sole peak appeared at 933 eV proves the formation of Cu₂O-NPs, in which Cu in chemical state Cu⁺ has been participated.

Scanning electron microscopy (SEM) and transmission electron microscopy (TEM) were used to investigate the size, morphology, and composition

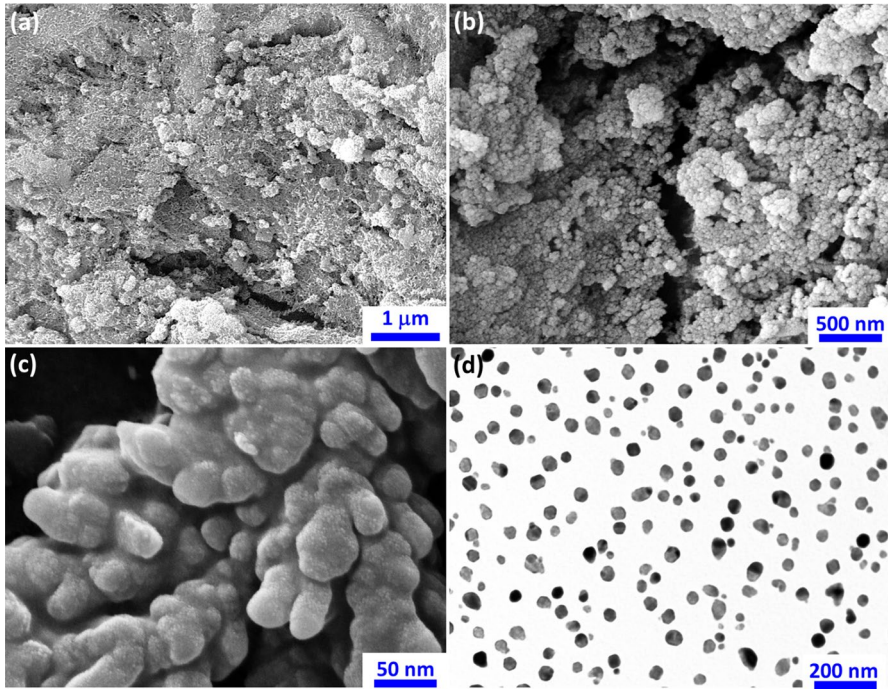


Fig. 5 a–c SEM image and d TEM image of the prepared Cu-ZnFe₂O₄@carrageenan nanocomposite

attitude of the prepared Cu-ZnFe₂O₄@carrageenan. As illustrated in the SEM image (Fig. 5a–c), the polymeric texture of the carrageenan substrate has been well-modified by the metallic NPs. Bright areas in the image (a) indicate that the metallic NPs have been successfully incorporated into the carrageenan matrix. Images (b and c) illustrate well-distribution of the metallic NPs onto the carrageenan textures with high magnification. As is observed in the image (c), the mean size of the formed NPs is ca. 47 nm. The same sample was investigated by TEM as well (Fig. 5d), and it was revealed that the ZnFe₂O₄ and Cu₂O-NPs have been well-distributed between the carrageenan textures. From the TEM image, it was also disclosed that the spherical-shaped NPs have been well-synthesized because high uniformity in size and morphology is observed for the particles. From these analyses, this is observed that well-dispersion of the metallic particles have been obtained despite of high magnetic behavior of Fe₂O₄-NPs. In fact, no agglomeration is observed for the ZnFe₂O₄ and Cu₂O-NPs, which is considered as a great point especially in catalytic applications. As shown in Fig. 5d, the mean size of the metallic particles is ca. 28 nm diameter, meaning that an extreme active surface area is provided by using a small amount of the particles. As is observed in TEM image, some of the heterogeneous particles have been formed of two sections, which are distinguished by light gray and dark gray colors. In this case, light and dark areas are attributed to Fe₂O₄ and Zn-NPs, respectively. The reason is related to more electronic density around the core of Zn atom that inhibits transmission of the electron beam of TEM instrument.

Catalytic application of Cu-ZnFe₂O₄@carrageenan nanocatalyst in xanthenedione derivatives

Optimization

To obtain the most appropriate conditions, various catalytic ratios of Cu-ZnFe₂O₄@carrageenan in different media and temperatures have been experimented for the catalyzed synthesis of 2,2'-(4-chlorophenyl methylene)bis(3-hydroxycyclohex-2-en-1-one) as a model reaction. The control reactions were tested in different times as well. Moreover, the efficiency of the individual carrageenan and ZnFe₂O₄ was compared with Cu-ZnFe₂O₄@carrageenan composite. As given in Table 1, the highest reaction yield is obtained when 0.01 g of the catalytic system has been applied in water medium during 10 min stirring under reflux conditions. Also, a gram-scale experiment was carried out to investigate the catalytic performance of the fabricated Cu-ZnFe₂O₄@carrageenan nanocatalyst in high scales. For this purpose, 10 mmol of each reactant and 0.1 g of the catalytic system were considered for doing the reaction, under optimal conditions. As can be observed in Table 1 (entry 12), 86% yield was obtained in totally 10 min, which is quite satisfying at this scale.

Table 1 Optimization of the catalytic process of the synthesis of 2,2'-(4-chlorophenyl methylene)bis(3-hydroxycyclohex-2-en-1-one)

Entry	Catalyst	Cat. W. (g)	Solvent	Temp. (°C)	Time (min)	Yield ^a (%)
1	–	–	H ₂ O	r.t	480	Trace
2	–	–	H ₂ O	Reflux	300	47
3	ZnFe ₂ O ₄	0.01	H ₂ O	Reflux	180	55
4	Carrageenan	0.01	H ₂ O	Reflux	180	70
5	Cu-ZnFe ₂ O ₄ @carrageenan	0.005	H ₂ O	Reflux	10	72
6	Cu-ZnFe ₂ O ₄ @carrageenan	0.01	H ₂ O	Reflux	10	98*
7	Cu-ZnFe ₂ O ₄ @carrageenan	0.02	H ₂ O	Reflux	10	98
8	Cu-ZnFe ₂ O ₄ @carrageenan	0.01	EtOH	Reflux	15	91
9	Cu-ZnFe ₂ O ₄ @carrageenan	0.01	THF	Reflux	90	73
10	Cu-ZnFe ₂ O ₄ @carrageenan	0.01	CH ₂ Cl ₂	Reflux	150	60
11	Cu-ZnFe ₂ O ₄ @carrageenan	0.01	H ₂ O/EtOH	Reflux	10	98
12	Cu-ZnFe ₂ O ₄ @carrageenan	0.01	DMSO	Reflux	10	78
13	Cu-ZnFe ₂ O ₄ @carrageenan	0.01	DMF	Reflux	10	82
14	Cu-ZnFe ₂ O ₄ @carrageenan	0.01	CH ₃ CN	Reflux	10	80
15	Cu-ZnFe ₂ O ₄ @carrageenan	0.01	H ₂ O	40	10	74
16	Cu-ZnFe ₂ O ₄ @carrageenan	0.1	H ₂ O	Reflux	10	86 ^b

*optimal conditions

^aIsolated yields. The conditions were monitored for the synthesis of 2,2'-(4-chlorophenyl methylene)bis(3-hydroxycyclohex-2-en-1-one), using 4-chlorobenzaldehyde (1.0 mmol), 1,3-cyclohexanedione or dimedone (2.0 mmol), and 2.0 mL solvent. The reaction progress was screened by thin-layer chromatography (elution solvent: a mixture of EtOAc and n-hexane [1:8])

^bgram-scale experiment

The catalytic activity of Cu-ZnFe₂O₄@carrageenan nanocatalyst

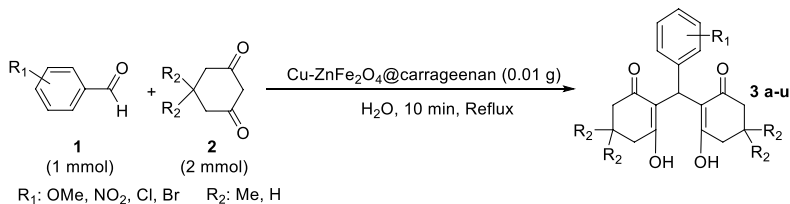
The capability of the prepared catalytic system was more investigated using various derivatives of aldehyde to synthesize different derivatives of xanthenedione. All of the reactions were carried out in the obtained optimal conditions. As given in Table 2, high reaction yields were obtained through applying a small amount of Cu-ZnFe₂O₄@carrageenan nanocatalyst. As the first and foremost excellence of our novel designed catalytic system well-applicability in the aqueous medium could be mentioned. In the other words, using this natural-based catalytic system is in great correspondence with the green chemistry principles. However, after obtaining the pure xanthenedione compounds, FT-IR and NMR spectroscopy were used to identify the structures [71]. Actually, the presence of the electron-withdrawing groups (EWG) onto the benzene ring accelerates the reaction because they make the aldehyde more activated and ready for reception of the nucleophiles. According to the literature and the obtained results in our study (Table 2), higher reaction yields are obtained for EWG-containing structures than the electron-donor groups like methoxy group [52, 53].

Proposed mechanism

Scheme 2 presents a plausible mechanism for catalyzed synthesis of xanthenedione derivatives. According to the literature, Cu and Zn present in the structure of catalyst activate the aldehyde component at the first stage [80]. Next, dimedone or 1,3-cyclohexanedione attacks to the activated aldehyde [81, 82]. At third stage, a dehydration process is performed to provide a conjugated unsaturated structure [83, 84]. Finally, a 1,4-addition is performed by another dimedone or 1,3-cyclohexanedione and the desired xanthenedione structure is formed [85, 86]. After completion of the process, the magnetic particles of the catalyst are regenerated and could be reused.

Recyclability of Cu-ZnFe₂O₄@carrageenan nanocomposite

To investigate recyclability of the catalytic system, the particles were separated after completion of the reaction of the synthesis of 2,2'-(4-chlorophenyl methylene)bis(3-hydroxycyclohex-2-en-1-one) **3u** and reused for additional five times. As shown in Fig. 6, the obtained reaction yield has been 10% reduced after five times recycling but is acceptable yet. For this purpose, the particles were conveniently collected using an external magnet, washed, and dried in oven. The FT-IR and EDX spectra of the recovered NPs have been prepared and illustrated in the supporting information section (Figs. S1 and S2). To investigate physisorption isotherms of the structure of Cu-ZnFe₂O₄@carrageenan nanocomposite, Brunauer–Emmett–Teller (BET) surface area analysis was carried out on the fresh catalyst and after recovering, via adsorption/desorption of N₂ gas (Fig. 7). The reversible isotherm of both and recovered catalyst is a typical type II, which is related to macroporous materials. The prepared Cu-ZnFe₂O₄@carrageenan nanocomposite has shown the type IV isotherm of mesoporous materials (pore size 2–50 nm) (Fig. 7b) with a hysteric loop in the

Table 2 Xanthenedione derivatives produced via the catalyzed synthetic process by Cu-ZnFe₂O₄@carrageenan nanocatalyst

Entry	Product structure	Product No	Yield ^a (%)	MP (°C)		Ref
				Found	Lit	
1	<p>2,2'-((2-chlorophenyl)methylene) bis(3-hydroxycyclohex-2-en-1-one)</p>	3a	93	226–229	229–231	[72]
2	<p>2,2'-((4-chlorophenyl)methylene) bis(3-hydroxycyclohex-2-en-1-one)</p>	3b	94	205–207	204	[73]
3	<p>2,2'-((3-chlorophenyl)methylene) bis(3-hydroxycyclohex-2-en-1-one)</p>	3c	93	202–204	199–200	[74]
4	<p>2,2'-((2-nitrophenyl)methylene) bis(3-hydroxycyclohex-2-en-1-one)</p>	3d	90	210–213	213	[73]

Table 2 (continued)

Entry	Product structure	Product No	Yield ^a (%)	MP (°C)		Ref
				Found	Lit	
<p> R_1: OMe, NO₂, Cl, Br R_2: Me, H </p>						
5	<p>2,2'-((3,4,5-trimethoxyphenyl)methylene) bis(3-hydroxycyclohex-2-en-1-one)</p>	3e	87	229–231	231–232	[74]
6	<p>2,2'-((2-methoxyphenyl)methylene) bis(3-hydroxycyclohex-2-en-1-one)</p>	3f	85	193–194	190–191	[74]
7	<p>2,2'-((3-nitrophenyl)methylene) bis(3-hydroxycyclohex-2-en-1-one)</p>	3g	93	204–206	207	[73]
8	<p>2,2'-((4-methoxyphenyl)methylene) bis(3-hydroxycyclohex-2-en-1-one)</p>	3h	89	194–197	197	[73]

Table 2 (continued)

Entry	Product structure	Product No	Yield ^a (%)	MP (°C)		Ref
				Found	Lit	
<p>Reaction scheme showing the synthesis of bis(3-hydroxy-2-en-1-one) derivatives (3 a-u) from aldehyde 1 and 1,3-dicarbonyl 2 using Cu-ZnFe₂O₄@carrageenan (0.01 g) in H₂O at reflux for 10 min. R₁: OMe, NO₂, Cl, Br; R₂: Me, H.</p>						
9	<p>2,2'-(phenylmethylene) bis(3-hydroxycyclohex-2-en-1-one)</p>	3i	90	218–220	219	[73]
10	<p>2,2'-((2-bromophenyl)methylene) bis(3-hydroxycyclohex-2-en-1-one)</p>	3j	90	196–198	199–200	[74]
11	<p>2,2'-(phenylmethylene)bis(3-hydroxy- 5,5-dimethylcyclohex-2-en-1-one)</p>	3k	90	194–197	196	[73]
12	<p>2,2'-((2-chlorophenyl)methylene)bis (3-hydroxy-5,5-dimethylcyclohex-2-en-1-one)</p>	3l	94	200–202	200	[73]
13	<p>2,2'-((2-nitrophenyl)methylene)bis (3-hydroxy-5,5-dimethylcyclohex-2-en-1-one)</p>	3m	94	188–190	191–193	[75]

Table 2 (continued)

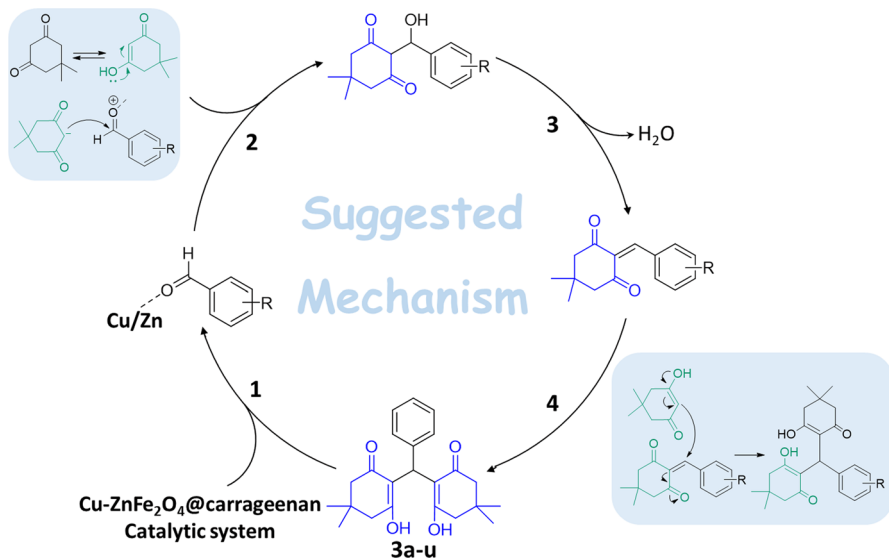
Entry	Product structure	Product No	Yield ^a (%)	MP (°C)		Ref
				Found	Lit	
<p>Reaction scheme showing the synthesis of bis-cyclohex-2-en-1-one derivatives (3 a-u) from substituted benzaldehyde (1) and substituted cyclohex-2-en-1-one (2) using Cu-ZnFe₂O₄@carrageenan (0.01 g) in H₂O, 10 min, Reflux. R₁: OMe, NO₂, Cl, Br; R₂: Me, H.</p>						
14	<p>2,2'-((2-methoxyphenyl)methylene)bis (3-hydroxy-5,5-dimethylcyclohex-2-en-1-one)</p>	3n	88	186–187	185	[73]
15	<p>2,2'-((3,4,5-trimethoxyphenyl)methylene)bis (3-hydroxy-5,5-dimethylcyclohex-2-en-1-one)</p>	3o	92	201–203	203–205	[76]
16	<p>2,2'-((3-chlorophenyl)methylene)bis (3-hydroxy-5,5-dimethylcyclohex-2-en-1-one)</p>	3p	95	183–185	184–186	[77]
17	<p>2,2'-((3-nitrophenyl)methylene)bis (3-hydroxy-5,5-dimethylcyclohex-2-en-1-one)</p>	3q	92	190–191	190	[78]

Table 2 (continued)

Entry	Product structure	Product No	Yield ^a (%)	MP (°C)		Ref
				Found	Lit	
<p> R_1: OMe, NO₂, Cl, Br R_2: Me, H </p>						
18	<p>2,2'-((3-methoxyphenyl)methylene)bis(3-hydroxy-5,5-dimethylcyclohex-2-en-1-one)</p>	3r	88	198–201	199–201	[74]
19	<p>2,2'-((4-methoxyphenyl)methylene)bis(3-hydroxy-5,5-dimethylcyclohex-2-en-1-one)</p>	3s	90	145–146	145	[73]
20	<p>2,2'-((2,4-dichlorophenyl)methylene)bis(3-hydroxy-5,5-dimethylcyclohex-2-en-1-one)</p>	3t	98	190–192	190–192	[79]
21	<p>2,2'-((4-chlorophenyl)methylene)bis(3-hydroxy-5,5-dimethylcyclohex-2-en-1-one)</p>	3u	98	142–144	145	[73]

^aIsolated yields

*All reactions were carried out in the optimum conditions (10 min)



Scheme 2 Plausible mechanism for the synthesis of xanthenedione derivatives, catalyzed by Cu-ZnFe₂O₄@carrageenan nanocomposite

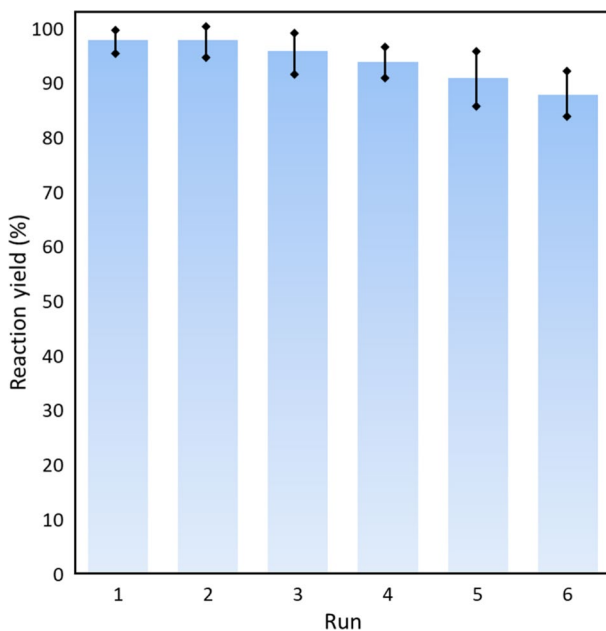


Fig. 6 Recycling diagram of Cu-ZnFe₂O₄@carrageenan nanocomposite in the synthesis reaction of **3u**

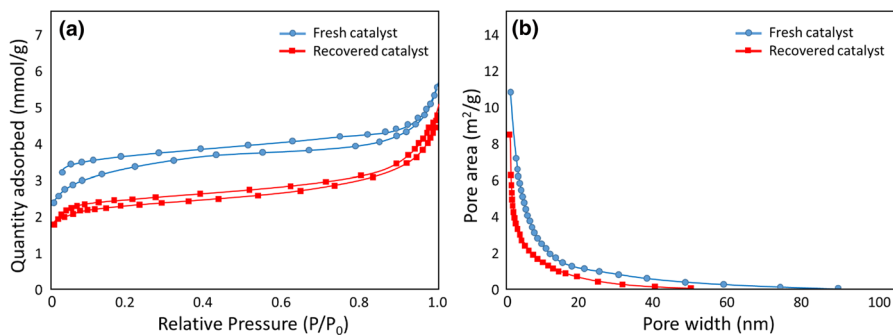


Fig. 7 **a** Isotherm linear plot, and **b** adsorption cumulative pore volume of Cu-ZnFe₂O₄@carrageenan nanocomposite before (blue) and after (red) the recycling process (circle-spotted curve: fresh catalyst, and square-spotted curve: recovered catalyst). (Color figure online)

range from 0.0 to 1.0 P/P_0 (Fig. 7a). From the curves, this is observed that the capacity of the pore sizes has been partially decreased after several times recycling, and as a result it can be expressed that the six times recovering has no significant effect on the porosity of the Cu-ZnFe₂O₄@carrageenan catalyst.

Comparison of catalyst

The efficiency of the Cu-ZnFe₂O₄@carrageenan nanocomposite was compared with previously reported catalytic systems in the literature. In Table 3, the synthesis of 2,2'-(4-chlorophenyl methylene)bis(3-hydroxycyclohex-2-en-1-one) **3u** in the presence of the Cu-ZnFe₂O₄@carrageenan nanocomposite is compared with other catalysts based on the reaction time (entries 1, 2 and 3) and the obtained yields (entries 1 and 2). As can be seen, the presented Cu-ZnFe₂O₄@carrageenan system well-works in a shorter time and results in higher yields than the previous catalysts.

Table 3 Comparison of Cu-ZnFe₂O₄@carrageenan nanocomposite with other previous systems

Entry	Cat. system	Conditions	Time (min)	Yield (%)	Ref
1	ZnO	CH ₃ CN/reflux	480	90	[87]
2	Copper (0) nanoparticles onto silica	EtOH/80 °C	60	93	[88]
3	Nano Fe/NaY Zeolite	EtOH/78 °C	70	98	[89]
4	CaCl ₂ (20% mmol)	CH ₃ Cl ₃ /r.t	840	79	[76]
5	Nanostructured Na ₂ CaP ₂ O ₇	H ₂ O/reflux	10	90	[77]
6	PVP ^a -Ni	Ethylene glycol/r.t	10	92	[78]
7	Fe ₃ O ₄ @SiO ₂ -SO ₃ H	H ₂ O/r.t	80	83	[90]
8	AOT ^b	Microwave irradiation	5	90	[91]
9	Cu-ZnFe ₂ O ₄ @carrageenan	H ₂ O/reflux	10	98	This work

^apolyvinyl pyrrolidone

^bsodiumbis -2-ethyl hexyl sulfosuccinate

Experimental

Materials and equipment

All of the applied materials and apparatuses are reported in Table S1 (SI section).

Methods

Preparation of ZnFe₂O₄@carrageenan nanocomposite

In a glass round-bottom flask (50 mL), Zn(NO₃)₂·6H₂O (0.6 g, 3.0 mmol) and Fe(NO₃)₃·9H₂O (1.6 g, 4.0 mmol) were mixed in deionized water (10 mL) via stirring at room temperature. Then, carrageenan (0.5 g) was added and the mixture was ultrasonicated for 40 min at 50 °C. Next, NaOH solution (0.1 M, 10 mL) was dropwise added into the flask until the mixture color was changed to dark brown that indicates formation of the ZnFe₂O₄ NPs successfully (pH ~ 12 is obtained). In continue, the reaction mixture was refluxed for 2 h. Finally, the obtained precipitation was magnetically separated, washed two times with water and ethanol, and dried at 78 °C [18, 47].

Preparation of Cu-ZnFe₂O₄@carrageenan nanocomposite

In a glass flask (100 mL), ZnFe₂O₄@carrageenan nanocomposite (0.5 g) was dispersed in ethanol (25 mL) and ascorbic acid (25 ml, 0.05 M, in deionized water), via ultrasonication for 30 min. Then, CuCl₂·2H₂O (0.5 mmol, 0.09 g) was added and the mixture was refluxed for 48 h. Finally, the obtained precipitation was prepared according to the procedure explained in the previous section [92, 93].

General procedure for catalysis of the synthesis reactions of xanthenedione derivatives 3a-u

In a glass round-bottom flask (25 mL), aldehyde derivative (1.0 mmol) and dimedone (or 1,3-cyclohexanedione) (2.0 mmol) were dissolved in deionized water (2.0 mL), and 0.01 g of Cu-ZnFe₂O₄@carrageenan nanocomposite was then added. Next, the mixture was exposed to ultrasound waves (50 kHz, 100 W L⁻¹) using a cleaner ultrasound bath, at room temperature (for 2 min). Afterward, the reaction mixture was refluxed for 10 min. Then, the catalyst particles were magnetically separated and 3.0 mL of deionized water was added. Afterward, DCM (5.0 mL) was added and extraction was carried out by using decanter. Finally, desired products were purified using flash-chromatography.

Spectral data for selected compounds

Product 3a (2,2'-(2-chlorophenyl)methylene)bis(3-hydroxycyclohex-2-en-1-one)
¹³CNMR (75 MHz, CDCl₃): δ (ppm) = 20.6, 28.9, 32.4, 37.2, 101.6, 123.6, 126.7, 127.7, 131.8, 132.2, 142.7, 196.2, 198.4. EI-MS [M]: m/z 348.

Product 3b (2,2'-((4-chlorophenyl)methylene)bis(3-hydroxycyclohex-2-en-1-one))
¹³CNMR (75 MHz, CDCl₃): δ (ppm)=20.0, 32.6, 33.0, 33.5, 116.1, 119.6, 128.4, 131.2, 137.0, 190.9, 192.2. EI-MS [M]: m/z 348.

Product 3c (2,2'-((3-chlorophenyl)methylene)bis(3-hydroxycyclohex-2-en-1-one))
¹³CNMR (75 MHz, CDCl₃): δ (ppm)=20.1, 32.8, 33.0, 33.5, 115.9, 122.5, 125.2, 129.0, 129.6, 129.7, 140.6, 190.9, 192.2. EI-MS [M]: m/z 348.

Product 3d (2,2'-((2-nitrophenyl)methylene)bis(3-hydroxycyclohex-2-en-1-one))
¹³CNMR (75 MHz, CDCl₃): δ (ppm)=21.1, 30.4, 34.1, 37.2, 108.1, 124.8, 129.1, 130.4, 134.5, 149.7, 190.1, 194.2. EI-MS [M]: m/z 357.

Product 3e (2,2'-((3,4,5-trimethoxyphenyl)methylene)bis(3-hydroxycyclohex-2-en-1-one))
¹³CNMR (75 MHz, CDCl₃): δ (ppm)=20.7, 33.2, 34.8, 36.7, 55.4, 59.2, 107.8, 109.5, 136.2, 136.5, 152.0, 180.2, 189.2. EI-MS [M]: m/z 402.

Product 3f (2,2'-((2-methoxyphenyl)methylene)bis(3-hydroxycyclohex-2-en-1-one))
¹³CNMR (75 MHz, CDCl₃): δ (ppm)=23.1, 29.6, 30.4, 33.8, 37.2, 50.4, 114.8, 121.9, 123.3, 125.4, 129.7, 147.1, 188.6, 193.2. EI-MS [M]: m/z 342.

Product 3g (2,2'-((3-nitrophenyl)methylene)bis(3-hydroxycyclohex-2-en-1-one))
¹³CNMR (75 MHz, CDCl₃): δ (ppm)=19.7, 20.3, 28.6, 32.8, 34.6, 36.4, 58.8, 100.1, 114.6, 120.4, 123.0, 128.7, 135.6, 147.1, 147.4, 168.5, 195.5, 199.1. EI-MS [M]: m/z 357.

Product 3h (2,2'-((4-methoxyphenyl)methylene)bis(3-hydroxycyclohex-2-en-1-one))
¹³CNMR (75 MHz, CDCl₃): δ (ppm)=20.1, 32.2, 33.0, 33.5, 55.2, 113.6, 116.6, 127.5, 129.7, 157.6, 190.8, 192.0. EI-MS [M]: m/z 342.

Product 3i (2,2'-((phenyl)methylene)bis(3-hydroxycyclohex-2-en-1-one))
¹³CNMR (75 MHz, CDCl₃): δ (ppm)=20.13, 32.92, 32.99, 33.51, 116.45, 125.85, 126.48, 128.16, 128.50, 130.18, 133.70, 138.18, 189.79, 191.82; EI-MS [M]: m/z 312.

Product 3j (2,2'-((2-bromophenyl)methylene)bis(3-hydroxycyclohex-2-en-1-one))
¹³CNMR (75 MHz, CDCl₃): δ (ppm)=21.2, 31.9, 33.7, 36.2, 112.4, 124.1, 127.3, 128.6, 130.9, 133.3, 146.3, 193.1, 195.7; EI-MS [M]: m/z 393.

Product 3k (2,2'-((phenyl)methylene)bis(3-hydroxy-5,5-dimethylcyclohex-2-en-1-one))
¹HNMR (300 MHz, CDCl₃): δ (ppm)=1.12 (s, 6H, 2CH₃), 1.25 (s, 6H, 2CH₃), 2.30–2.50 (m, 8H, 4CH₂), 5.56 (s, 1H, CH), 7.10–7.30 (m, 4H, H-Ar), 11.92 (s, 1H, OH). ¹³CNMR (75 MHz, CDCl₃): δ (ppm)=27.2, 29.6, 31.4, 32.74, 46.5, 47.0, 115.6, 125.5, 126.7, 128.2, 138.5, 189.4, 190.8. EI-MS [M]: m/z 368.

Product 3l (2,2'-((2-chlorophenyl)methylene)bis(3-hydroxy-5,5-dimethylcyclohex-2-en-1-one))
¹HNMR (300 MHz, CDCl₃): δ (ppm)=1.06 (s, 6H, 2CH₃), 1.33 (s, 6H, 2CH₃), 2.06–2.50

(m, 8H, 4CH₂), 5.57 (s, 1H, CH), 7.00–7.52 (m, 4H, H-Ar), 11.90 (s, 1H, OH). ¹³C NMR (75 MHz, CDCl₃): δ (ppm)=27.4, 28.9, 29.5, 31.3, 46.4, 46.2, 115.5, 115.5, 115.7, 125.1, 125.5, 127.9, 127.9, 129.1, 129.2, 159.1, 162.6, 189.5. EI-MS [M]: m/z 404.

Product 3 m (2,2'-(2-nitrophenyl)methylene)bis(3-hydroxy-5,5-dimethylcyclohex-2-en-1-one) ¹H NMR (300 MHz, CDCl₃): δ (ppm)=1.02 (s, 6H, 2CH₃), 1.17 (s, 6H, 2CH₃), 2.25–2.54 (m, 8H, 4CH₂), 6.05 (s, 1H, CH), 7.27 (d, 1H, H-Ar), 7.28 (t, 1H, H-Ar), 7.47 (t, 1H, H-Ar), 7.57 (d, 1H, H-Ar), 11.60 (s, 1H, OH). ¹³C NMR (75 MHz, CDCl₃): δ (ppm)=28.4, 28.3, 30.5, 31.9, 46.3, 46.4, 114.4, 124.3, 127.7, 129.5, 131.3, 132.1, 149.2, 189.0, 191.2. EI-MS [M]: m/z 413.

Product 3 n (2,2'-(2-methoxyphenyl)methylene)bis(3-hydroxy-5,5-dimethylcyclohex-2-en-1-one) ¹H NMR (300 MHz, CDCl₃): δ (ppm)=1.12 (s, 6H, 2CH₃), 1.35 (s, 6H, 2CH₃), 3.73–3.79 (m, 8H, 4CH₂), 5.59 (s, 1H, CH), 6.80–7.28 (m, 4H, H-Ar), 11.86 (s, 1H, OH). ¹³C NMR (75 MHz, CDCl₃): δ (ppm)=29.2, 31.2, 46.2, 55.8, 116.4, 119.9, 126.1, 127.0, 128.5, 157.1, 189.2. EI-MS [M]: m/z 398.

Product 3 o (2,2'-(3,4,5-trimethoxyphenyl)methylene)bis(3-hydroxy-5,5-dimethylcyclohex-2-en-1-one) ¹³C NMR (75 MHz, CDCl₃): δ (ppm)=27.2, 32.9, 35.6, 38.9, 51.3, 57.2, 60.7, 106.8, 108.2, 136.4, 137.3, 151.2, 182.0, 190.8. EI-MS [M]: m/z 458.

Product 3 p (2,2'-(3-chlorophenyl)methylene)bis(3-hydroxy-5,5-dimethylcyclohex-2-en-1-one) ¹H NMR (300 MHz, CDCl₃): δ (ppm)=0.89 (s, 6H, 2CH₃), 1.09 (s, 6H, 2CH₃), 2.10–2.39 (m, 8H, 4CH₂), 5.59 (s, 1H, CH), 7.20–7.40 (m, 4H, H-Ar), 11.89 (s, 1H, OH). ¹³C NMR (75 MHz, CDCl₃): δ (ppm)=27.7, 29.13, 32.1, 34.1, 47.8, 50.9, 111.9, 124.7, 128.7, 131.4, 135.4, 144.3, 189.9, 191.7. EI-MS [M]: m/z 404.

Product 3 q (2,2'-(3-nitrophenyl)methylene)bis(3-hydroxy-5,5-dimethylcyclohex-2-en-1-one) ¹H NMR (300 MHz, CDCl₃): δ (ppm)=1.12 (s, 6H, 2CH₃), 1.28 (s, 6H, 2CH₃), 2.32–2.53 (m, 8H, 4CH₂), 5.54 (s, 1H, CH), 7.26–8.05 (m, 4H, H-Ar), 11.87 (s, 1H, OH). ¹³C NMR (75 MHz, CDCl₃): δ (ppm)=27.3, 29.7, 31.4, 32.9, 46.4, 47.0, 114.8, 121.0, 122.2, 129.1, 132.9, 140.7, 148.4, 189.6, 191.1. EI-MS [M]: m/z 413.

Product 3 r (2,2'-(3-methoxyphenyl)methylene)bis(3-hydroxy-5,5-dimethylcyclohex-2-en-1-one) ¹³C NMR (75 MHz, CDCl₃): δ (ppm)=27.8, 29.9, 32.5, 34.6, 47.5, 51.2, 55.8, 114.7, 121.1, 123.8, 129.6, 148.6, 160.4, 187.9, 192.1. EI-MS [M]: m/z 398.

Product 3 s (2,2'-(4-methoxyphenyl)methylene)bis(3-hydroxy-5,5-dimethylcyclohex-2-en-1-one) ¹³C NMR (75 MHz, CDCl₃): δ (ppm)=27.0, 29.3, 31.1, 31.8, 40.5, 46.2, 46.8, 50.5, 54.9, 113.4, 115.5, 127.5, 129.0, 130.2, 157.3, 161.8, 189.0, 190.0. EI-MS [M]: m/z 398.

Product 3t (2,2'-((2,4-dichlorophenyl)methylene)bis(3-hydroxy-5,5-dimethylcyclohex-2-en-1-one)) ^1H NMR (300 MHz, CDCl_3): δ (ppm)=1.01 (s, 6H, 2CH_3), 1.38 (s, 6H, 2CH_3), 2.22–2.44 (m, 8H, 4CH_2), 5.49 (s, 1H, CH), 6.58–7.27 (m, 4H, H-Ar), 11.95 (s, 1H, OH). ^{13}C NMR (75 MHz, CDCl_3): δ (ppm)=27.8, 29.4, 31.6, 32.7, 46.2, 47.4, 114.2, 126.9, 129.0, 129.8, 130.0, 132.3, 138.7, 189.4, 190.7. EI-MS [M]: m/z 436.

Product 3u (2,2'-((4-chlorophenyl)methylene)bis(3-hydroxy-5,5-dimethylcyclohex-2-en-1-one)) ^1H NMR (300 MHz, CDCl_3): δ (ppm)=1.11 (s, 6H, 2CH_3), 1.32 (s, 6H, 2CH_3), 2.19–2.50 (m, 8H, 4CH_2), 5.48 (s, 1H, CH), 7.01–7.28 (m, 4H, H-Ar), 11.88 (s, 1H, OH). ^{13}C NMR (75 MHz, CDCl_3): δ (ppm)=27.2, 29.5, 31.4, 32.4, 46.4, 47.0, 115.3, 128.2, 128.3, 131.5, 136.7, 189.4, 190.6. EI-MS [M]: m/z 404.

Conclusions

In summary, a novel hybrid heterogeneous catalytic system has been prepared from carrageenan as a natural polymeric matrix for immobilization of the ZnFe_2O_4 and Cu_2O NPs, and applied for convenient synthesis of xanthenedione pharmaceutical derivatives. Herein, the chemical structure and physical properties of the prepared mixed transition metal oxides catalytic system ($\text{Cu-ZnFe}_2\text{O}_4$ @carrageenan) have been studied by various analyses. Briefly, well-composition of three components has been confirmed by FT-IR and EDX spectroscopy. From EDX, it has been revealed that 4.45 wt% Cu is incorporated into the structure of the composite, which are the main active catalytic sites. Moreover, high heterogeneity and structural stability of the fabricated $\text{Cu-ZnFe}_2\text{O}_4$ @carrageenan have been proven by TGA. Besides, great magnetic property of the catalyst has been shown by magnetic hysteresis (M-H) curves. These substantial features make the presented catalytic system as an instrumental recoverable tool for organic catalysis. In this report, it has been revealed that a six-time successive recycling and reuse does not negatively influence on the catalytic performance and no structural deterioration is observed. Furthermore, uniform distribution of the Cu_2O NPs (in ca. 28 nm mean size) onto the carrageenan textures has been demonstrated by SEM and TEM methods. X-ray-based analytical methods such as XRD and XPS have revealed the successful formation of Cu(I), as well. However, the catalytic activity of this nanoscale catalyst has been investigated in the synthesis of the various derivatives of xanthenedione. In this work, it has been demonstrated that high reaction yields (above 90%) are obtained in short time (10 min) through using $\text{Cu-ZnFe}_2\text{O}_4$ @carrageenan heterogeneous catalytic system. In addition, due to high convenience in the separation and purification process (through the magnetic property) and great recyclability of $\text{Cu-ZnFe}_2\text{O}_4$ @carrageenan, this novel designed catalytic system is suggested for industrial applications.

Supplementary data

The SI file includes the NMR of selected xanthenedione products. The brand and purity of the used materials have also been listed in this section. This section can be found in the online version.

Acknowledgements The authors gratefully acknowledge the partial support from the Research Council of the Iran University of Science and Technology (IUST).

Compliance with ethical standards

Conflict of interest The authors declare no conflict of interest.

References

- J.C. Garrison, C.A. Tessier, W.J. Youngs, *J. Organomet. Chem.* **690**, 6008 (2005)
- R. Taheri-Ledari, S.M. Hashemi, A. Maleki, *RSC Adv.* **9**, 40348 (2019)
- M. Peng, C. Hong, Y. Huang, P. Cheng, H. Yuan, *J. Organomet. Chem.* **909**, 121110 (2016)
- L.V. Gelderen, G. Rothenberg, V.R. Calderone, K. Wilson, N.R. Shiju, *Appl. Organomet. Chem.* **27**, 23 (2013)
- R.K. Mondal, S. Riyajuddin, A. Ghosh, S. Ghosh, K. Ghosh, S.M. Islam, *J. Organomet. Chem.* **880**, 322 (2018)
- M.J. Alcón, A. Corma, M. Iglesias, F. Sánchez, *J. Organomet. Chem.* **655**, 134 (2002)
- J. Xu, H. Shimakoshi, Y. Hisaeda, *J. Organomet. Chem.* **2015**, 89 (2013)
- A. Bahuguna, A. Kumar, V. Krishnan, *Asian. J. Org. Chem.* **8**, 1263 (2019)
- M.B. Gawande, A. Goswami, F. Felpin, T. Asefa, X. Huang, R. Silva, X. Zou, R. Zboril, R.S. Varma, *Chem. Rev.* **116**, 3722 (2016)
- M.R. Khodabakhshi, M. Kiamehr, F.M. Moghaddam, A. Villinger, P. Langer, *ChemistrySelect* **3**, 1167 (2018)
- A. Maleki, R. Taheri-Ledari, R. Ghalavand, R. Firouzi-Haji, *J. Phys. Chem. Solids* **136**, 109200 (2020)
- J. Huang, S. Liu, Y. Ma, J. Cai, *J. Organomet. Chem.* **886**, 27 (2019)
- S. Layek, B. Agrahari, S. Dey, R. Ganguly, D.D. Pathak, *J. Organomet. Chem.* **896**, 194 (2019)
- H. Karimi, M.A. Heidari, H.B.M. Emrooz, M. Shokouhimehr, *Diam. Relat. Mater.* **108**, 107999 (2020)
- P. Nazari, M. Hekmati, *Appl. Organomet. Chem.* **33**, e4729 (2019)
- A. Maleki, M. Niksefat, J. Rahimi, R. Taheri-Ledari, *Mater. Today Chem.* **13**, 110 (2019)
- C. Boztepe, A. Künkül, S. Yaşar, N. Gürbüz, *J. Organomet. Chem.* **872**, 123 (2018)
- Z. Varzi, A. Maleki, *Appl. Organomet. Chem.* **32**, e5008 (2019)
- A. Martínez, C. Hemmert, H. Gornitzka, B. Meunier, *J. Organomet. Chem.* **690**, 2163 (2005)
- Y.A. Attia, Y.M.A. Mohamed, M.M. Awad, S. Alexeree, *J. Organomet. Chem.* **919**, 121320 (2020)
- J. Li, Y. Wang, S. Jiang, H. Zhang, *J. Organomet. Chem.* **878**, 84 (2018)
- J. Rahimi, R. Taheri-Ledari, M. Niksefat, A. Maleki, *Catal. Commun.* **134**, 105850 (2020)
- R. Taheri-Ledari, W. Zhang, M. Radmanesh, S.S. Mirmohammadi, A. Maleki, N. Cathcart, V. Kitaev, *Small* **16**, 2002733 (2020)
- N. Hazeri, A. Masoumnia, M.T. Mghsoodlou, S. Salahi, M. Kangani, S. Kianpour, S. Kiaee, J. Abonajmi, *Res. Chem. Intermed.* **41**, 4123 (2015)
- S.E.S. Sorkhi, M.M. Hashemi, A. Ezabadi, *Res. Chem. Intermed.* **46**, 2229 (2020)
- T.R.R. Naik, S.A. Shivashankar, *Tetrahedron Lett.* **57**, 4046 (2016)
- A. Habibi, M.H. Baghersad, M. Bilabary, Y. Valizadeh, *Tetrahedron Lett.* **57**, 559 (2016)
- S. Parvaz, R. Taheri-Ledari, M.S. Esmaeili, M. Rabbani, A. Maleki, *Life Sci.* **240**, 117099 (2020)
- H.Y. Lü, J.J. Li, Z.H. Zhang, *Appl. Organomet. Chem.* **23**, 165 (2009)
- M. Kidwai, A. Jain, *Appl. Organomet. Chem.* **26**, 528 (2012)

31. K. Valadi, S. Gharibi, R. Taheri-Ledari, A. Maleki, *Solid State Sci.* **101**, 106141 (2020)
32. V. Vatanpour, H. Karimi, S.I. Ghazanlou, Y. Mansourpanah, M.R. Ganjali, A. Badiei, E. Pourbashir, M.R. Saeb, *J. Environ. Chem. Eng.* **8**, 104454 (2020)
33. J. Akbari, A. Heydari, H.R. Kalhor, S.A. Kohan, *J. Comb. Chem.* **12**, 137 (2010)
34. R. Taheri-Ledari, A. Maleki, *J. Pept. Sci.* **26**, e3277 (2020)
35. H.S. Far, M. Hasanzadeh, M.S. Nashtaei, M. Rabbani, A. Haji, B.H. Moghadam, *A.C.S. Appl. Mater. Interfaces* **12**, 25294 (2020)
36. M.J. Iqbal, Z. Ahmad, Y. Melikho, I.C. Nlebedim, *J. Magn. Magn. Mater.* **324**, 1018 (2012)
37. A. Maleki, K. Valadi, S. Gharibi, R. Taheri-Ledari, *Res. Chem. Intermed.* **46**, 4113 (2020)
38. M. Mehdipour, M.R. Khodabakhshi, *Curr. Chem. Lett.* **9**, 9 (2020)
39. M.H. Baghersad, S. Jamshidi, A. Habibi, A. Salimi, *ChemistrySelect* **4**, 810 (2019)
40. N. Elahi, M. Kamali, M.H. Baghersad, B. Amimi, *Mater. Sci. Eng. C* **105**, 110113 (2019)
41. A. Maleki, R. Taheri-Ledari, M. Soroushnejad, *ChemistrySelect* **3**, 13057 (2018)
42. A. Maleki, R. Taheri-Ledari, J. Rahimi, M. Soroushnejad, Z. Hajizadeh, *ACS Omega* **4**, 10629 (2019)
43. R. Taheri-Ledari, J. Rahimi, A. Maleki, *Mater. Res. Express.* **7**, 015067 (2020)
44. R. Taheri-Ledari, A. Maleki, E. Zolfaghari, M. Radmanesh, H. Rabbani, A. Salimi, R. Fazel, *Ultrason. Sonochem.* **61**, 104824 (2020)
45. M.S. Esmaili, M.R. Khodabakhshi, A. Maleki, Z. Varzi, *Polycycl. Aromat. Compd.* (2020). <https://doi.org/10.1080/10406638.2019.1708418>
46. A. Maleki, F. Hassanzadeh-Afruzi, Z. Varzi, M.S. Esmaili, *Mater. Sci. Eng. C* **109**, 110502 (2020)
47. A. Maleki, Z. Varzi, F. Hassanzadeh-Afruzi, *Polyhedron* **171**, 193 (2019)
48. R. Taheri-Ledari, J. Rahimi, A. Maleki, *Ultrason. Sonochem.* **59**, 104737 (2019)
49. R. Eyvazzadeh-Keihan, N. Bahrami, R. Taheri-Ledari, A. Maleki, *Diam. Relat. Mater.* **102**, 107661 (2020)
50. H. Xie, H. Liu, M. Wang, H. Pan, C. Gao, *Appl. Organomet. Chem.* **34**, e5256 (2020)
51. M.J. Nejad, A. Salamatmanesh, A. Heydari, *J. Organomet. Chem.* **911**, 121128 (2020)
52. F.M. Moghaddam, A. Jarahiyan, M. Eslami, A. Pourjavadi, *J. Organomet. Chem.* **916**, 121266 (2020)
53. F. Rafiee, P. Khavari, Z. Payami, N. Ansari, *J. Organomet. Chem.* **883**, 78 (2019)
54. I. Yavari, A. Mobaraki, Z. Hosseinzadeh, N. Sakhaee, *J. Organomet. Chem.* **897**, 236 (2019)
55. M. Kumari, R. Gupta, Y. Jain, *Appl. Organomet. Chem.* **33**, e5223 (2019)
56. X. Meng, G. Li, H. Hou, H. Han, Y. Fan, Y. Zhu, C. Du, *J. Organomet. Chem.* **679**, 153 (2003)
57. C.J. Cheng, O.G. Jones, *Food Hydrocoll.* **69**, 28 (2017)
58. S. Rostamnia, B. Zeynizadeh, E. Doustkhah, A. Baghban, K.O. Aghbash, *Catal. Commun.* **68**, 77 (2015)
59. C. Cai, Z. Zhang, J. Liu, N. Shan, H. Zhang, D.D. Dionysiou, *Appl. Catal. B.* **182**, 456 (2006)
60. S. Soltani, U. Rashid, I. Arbi Nehdi, S.I. Al-Resayes, *Chem. Eng. Technol.* **40**, 1931 (2007)
61. W. Zhang, R. Taheri-Ledari, Z. Hajizadeh, E. Zolfaghari, M.R. Ahghari, A. Maleki, M.R. Hamblin, Y. Tian, *Nanoscale* **12**, 3855 (2020)
62. A. Maleki, S. Gharibi, K. Valadi, R. Taheri-Ledari, *J. Phys. Chem. Solids* **142**, 109443 (2020)
63. A. Maleki, R. Taheri-Ledari, R. Ghalavand, *Comb. Chem. High T. Scr.* **23**, 119 (2020)
64. A. Rasool, S. Ata, A. Islam, M. Rizwan, M.K. Azeem, A. Mehmood, R.U. Khan, A. Ur Rehman Qureshi, H. Arshad Mahmood, *Int. J. Biol. Macromol.* **147**, 67 (2020)
65. Y.Y. Tye, A.K. HPS, C.Y. Kok, C.K. Saurabh, *IOP Conference Series: Materials Science and Engineering*, WOBIC, Selangor, Malaysia. **368**, 21 (2017)
66. N. Ahmadpour, M.H. Sayadi, S. Sobhani, M. Hajiani, *J. Clean. Prod.* **268**, 122023 (2020)
67. G.R. Mahdavinia, H. Etemadi, *Arab. J. Chem.* **12**, 3692 (2019)
68. P. Sangeetha, T.M. Selvakumari, S. Selvasekarapandian, S.R. Srikumar, R. Manjuladevi, M. Mahalakshmi, *Ionics* **26**, 233 (2020)
69. P. Duan, R. Su, X. Xu, Q. Li, B. Gao, *J. Taiwan Inst. Chem. Eng.* **102**, 456 (2019)
70. S. Ghosh, S. Saha, D. Sengupta, S. Chattopadhyay, G. De, B. Basu, *Ind. Eng. Chem. Res.* **56**, 11726–11733 (2017)
71. C. Shen, H. Li, Y. Wen, F. Zhao, Y. Zhang, D. Wu, Y. Liu, F. Li, *Chem. Eng. J.* **383**, 123105 (2020)
72. J.K. Rajput, G. Kaur, *Catal. Sci. Technol.* **4**, 142 (2014)
73. S.H. Banakar, M.G. Dekamin, A. Yaghoubi, *New J. Chem.* **42**, 14246 (2018)
74. K.M. Khan, G.M. Maharvi, M.T.H. Khan, A.J. Shaikh, S. Perveen, S. Begum, M.I. Choudhary, *Med. Chem.* **14**, 344 (2006)

75. Y. Ren, B. Yang, X. Liao, *RSC Adv.* **6**, 22034 (2016)
76. A. Ilangovan, S. Muralidharan, P. Sakthivel, S. Malayappasamy, S. Karuppusamy, M.P. Kaushik, *Tetrahedron Lett.* **54**, 491 (2013)
77. B. Maleki, M. Raei, H. Alinezhad, R. Tayebee, A. Sedrpoushan, *Org. Prep. Proced. Int.* **50**, 288 (2018)
78. J.M. Khurana, K. Vij, J. Nickel, *Chem. Sci.* **124**, 907 (2012)
79. M.T. Maghsoodlou, S.M. Habibi-Khorassani, Z. Shahkarami, N. Maleki, M. Rostamizadeh, *Chin. Chem. Lett.* **21**, 7413 (2017)
80. R.G. Chaudhary, V.N. Sonkusare, G.S. Bhusari, A. Mondal, D.P. Shaik, H.D. Juneja, *Res. Chem. Intermed.* **44**, 2039 (2018)
81. M. Salami, A. Ezabadi, *Res. Chem. Intermed.* **46**, 4611 (2020)
82. N.G. Khaligh, *Res. Chem. Intermed.* **44**, 4045 (2018)
83. S. Karhale, M. Patil, G. Rashinkar, V. Helavi, *Res. Chem. Intermed.* **43**, 7073 (2017)
84. N. Mohammadian, B. Akhlaghinia, *Res. Chem. Intermed.* **44**, 1085 (2018)
85. M. Rahimifard, G.M. Ziarani, A. Badiei, S. Asadi, A.A. Soorki, *Res. Chem. Intermed.* **42**, 3847 (2016)
86. A. Fallah, M. Tajbakhsh, H. Vahedi, A. Bekhradnia, *Res. Chem. Intermed.* **43**, 29 (2017)
87. M.T. Maghsoodlou, S.M. Habibi-khorassani, Z. Shahkarami, N. Maleki, M. Rostamizadeh, *Chin. Chem. Lett.* **21**, 686 (2010)
88. M. Gupta, M. Gupta, *J. Chem. Sci.* **128**, 849 (2016)
89. M. Tajbakhsh, M. Heidary, *Res. Chem. Intermed.* **42**, 1425 (2016)
90. F. Nemat, M.M. Heravi, R.S. Rad, *Chin. J. Catal.* **33**, 1825 (2012)
91. M. Saha, J. Dey, K. Ismail, A.K. Pal, *Lett. Org. Chem.* **8**, 554 (2011)
92. M.S. Esmaeili, Z. Varzi, R. Eivazzadeh-Keihan, A. Maleki, H. Ghafuri, *Mol. Catal.* **492**, 111037 (2020)
93. S. Shaabani, A.T. Tabatabaei, A. Shaabani, *Appl. Organomet. Chem.* **31**, e3559 (2017)

Publisher's Note Springer Nature remains neutral with regard to jurisdictional claims in published maps and institutional affiliations.